

**Zeitschrift:** IABSE reports of the working commissions = Rapports des commissions de travail AIPC = IVBH Berichte der Arbeitskommissionen

**Band:** 34 (1981)

**Artikel:** Experiments and models for the damping behavior of vibrating reinforced concrete beams in the uncracked and cracked condition

**Autor:** Dieterle, R. / Bachman, H.

**DOI:** <https://doi.org/10.5169/seals-26880>

### **Nutzungsbedingungen**

Die ETH-Bibliothek ist die Anbieterin der digitalisierten Zeitschriften auf E-Periodica. Sie besitzt keine Urheberrechte an den Zeitschriften und ist nicht verantwortlich für deren Inhalte. Die Rechte liegen in der Regel bei den Herausgebern beziehungsweise den externen Rechteinhabern. Das Veröffentlichen von Bildern in Print- und Online-Publikationen sowie auf Social Media-Kanälen oder Webseiten ist nur mit vorheriger Genehmigung der Rechteinhaber erlaubt. [Mehr erfahren](#)

### **Conditions d'utilisation**

L'ETH Library est le fournisseur des revues numérisées. Elle ne détient aucun droit d'auteur sur les revues et n'est pas responsable de leur contenu. En règle générale, les droits sont détenus par les éditeurs ou les détenteurs de droits externes. La reproduction d'images dans des publications imprimées ou en ligne ainsi que sur des canaux de médias sociaux ou des sites web n'est autorisée qu'avec l'accord préalable des détenteurs des droits. [En savoir plus](#)

### **Terms of use**

The ETH Library is the provider of the digitised journals. It does not own any copyrights to the journals and is not responsible for their content. The rights usually lie with the publishers or the external rights holders. Publishing images in print and online publications, as well as on social media channels or websites, is only permitted with the prior consent of the rights holders. [Find out more](#)

**Download PDF:** 05.09.2025

**ETH-Bibliothek Zürich, E-Periodica, <https://www.e-periodica.ch>**

## **Experiments and Models for the Damping Behavior of Vibrating Reinforced Concrete Beams in the Uncracked and Cracked Condition**

Essais et modèles pour l'amortissement de poutres en béton armé dans l'état non-fissuré

Versuche und Modelle für das Dämpfungsverhalten schwingender Stahlbetonträger im ungerissenen und gerissenen Zustand

**R. DIETERLE**  
Research Associate  
Swiss Federal Institute of Technology  
Zurich, Switzerland

**H. BACHMAN**  
Prof. Dr.  
Swiss Federal Institute of Technology  
Zurich, Switzerland,

### **SUMMARY**

Different models for the damping behavior of normally reinforced, uncracked and cracked concrete beams and constructions under dominating bending stress are presented. By comparison with experimental results it can be shown that the results of the theoretical damping models are in good agreement with those of the experiments.

### **RÉSUMÉ**

On présente des modèles qui permettent de concevoir l'amortissement de poutres et constructions en béton non-fissurés et fissurés, soumis surtout à des sollicitations de flexion. Par comparaison avec des résultats déterminés à l'aide d'essais on montre, que l'emploi des modèles présentés donne des résultats concordants avec ceux des essais.

### **ZUSAMMENFASSUNG**

Es werden verschiedene Modelle für das Dämpfungsverhalten von schwingenden Stahlbetonträgern und -konstruktionen im ungerissenen und gerissenen Zustand, welche vorwiegend auf Biegung beansprucht werden, dargestellt. Anhand von Vergleichen mit experimentellen Resultaten wird die Anwendbarkeit der präsentierten Modelle aufgezeigt.



## 1. INTRODUCTION

Recently, the dynamic analysis of reinforced concrete structures has greatly increased in significance. Yet important knowledge in several areas is still lacking especially information concerning damping, which can decidedly influence a dynamic calculation.

The damping of reinforced concrete structures is based upon various and at times little-known physical causes, and depends upon numerous influencing parameters. It is therefore not surprising that in experiments the fixed values for the damping scatter within a broad range. The two chief causes for this scatter are as follows:

- The material damping of reinforced concrete building components and reinforced concrete constructions is influenced not only by the damping properties of the material used, but also strongly by the crack condition. For uncracked structures, especially fully prestressed uncracked structures, the damping properties in many cases can be described with closely agreeing values. For normally-reinforced and partly-prestressed structures, however, there exists in the literature a large variation both qualitatively and quantitatively with regard to the influence of the crack condition. Normally it is accepted that reinforced concrete structures in the cracked condition show in addition to low eigenfrequencies a considerable increase in damping in comparison to those in the uncracked condition.
- In general, the damping of an entire reinforced concrete construction is influenced not only by the material damping but also by the system damping, that is by the damping properties of the surroundings (building site, development of statical system, etc.). Since the fraction of the system damping on the total damping can be considerable, it is possible that analogous structures in different surroundings will show very different damping behaviors.

In order to check this behavior and to determine the influence of important construction parameters on the material damping properties of reinforced concrete, systematic experiments on seven normally-reinforced concrete and light-weight concrete beams were conducted at the Institute of Structural Engineering at the Swiss Federal Institute of Technology Zurich. These experiments and the achieved results are described in [1] and [2]. They provide the experimental groundwork for the theoretical work performed in [3]. The most important results of this work are put forth in the following report.

## 2. OBJECTIVES

The objectives of the described research project are as follows:

1. The determination of the influence of the crack condition, of the stress level and of the amount of reinforcement on the damping properties of normally-reinforced concrete and light-weight concrete beams.
2. The development of physically plausible and mathematically simple models which can not only explain the experimentally recorded damping phenomena on the test beams, but also can predict the material damping properties of more complex concrete and light-weight concrete constructions.

## 3. TESTS ON NORMALLY-REINFORCED CONCRETE BEAMS

In the experiments mentioned in the introduction, vibration and resonance tests were performed on seven concrete and light-weight concrete beams of varying longitudinal reinforcement. All beams had identical dimensions (length  $L = 8.40$  m, width  $B = 0.40$  m, depth  $H = 0.24$  m), and after cracking all had their first eigenfrequency in the range from 2 to 7 Hz. Briefly repeated here will be several results which give information on the established damping properties and which

are necessary for the disposition and understanding of the following report.

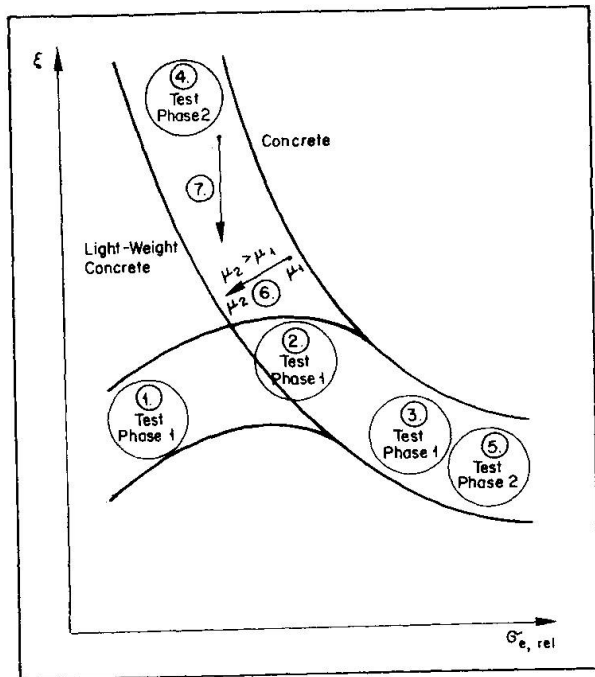


Fig. 1 Damping Ratio  $\xi$  as a Function of the Steel Stress  $\sigma_{e,rel}$  (schematic)

In Fig. 1, the established curve of the damping ratio as a function of the relative steel stress  $\sigma_{e,rel}$  in the middle of the beam is schematically shown for all test beams.

The index "rel" (= relative) signifies that the stress refers to the difference between the values measured in the dynamic test and in the at-rest state.

The established damping properties can be described as follows, with the numbering scheme referring to the numbering scheme of Fig. 1:

#### Initial Stressing and Cracking Phase

(test phase 1)

1. The damping for all beams increased during cracking (crack formation and spreading) following the increasing steel stress.
2. Approximately as soon as all bending cracks had formed, a condition was reached for which the damping ceased to increase further.
3. With the further increase in stress, respectively steel stress, the damping decreased. As the steel stresses neared the yield point, very small damping values were measured ( $\xi < 1\%$ ), especially for heavily-reinforced beams.

#### After Conclusion of Cracking and with Repeat of Testing

(test phase 2)

During the repeated execution of the total test program the following damping behavior for each of the beams could be observed:

4. A very high damping was established for small steel stresses, in contrast to test phase 1. For increasing steel stress, however, the damping again decreased.
5. Somewhat smaller values for the damping than in test phase 1 were measured for large steel stresses.
6. A lower damping was found for increasing amounts of reinforcement.
7. The light-weight concrete beams showed a lower damping ability over the entire stress range as the corresponding concrete beams.

The described results show that, contrary to the usual assumptions, the damping ratio as a result of cracking can sink to a very small value after an initial growth. Although this phenomenon appears surprising, it can nevertheless be explained in a physically plausible manner by the still-to-be-described damping models.



#### 4. EXPERIMENTS ON UNREINFORCED CONCRETE TEST BODIES

Numerous experiments for the determination of damping of unreinforced concrete test bodies are described in the literature ([4], [5], [6], [7], [8]). The following influence factors with regard to the damping of unreinforced concrete are considered:

- Water content of the concrete
- Age of the concrete
- Cement content of the concrete
- Frequency
- Level of stress

Many experimental investigations have shown that the cement content and the frequency have an insignificant influence on the damping. In addition it can be established that for small stresses ( $\sigma_b < \beta_w/2$ ), the stress level has practically no influence on the damping properties. However, the water content and, coupled with it, the age of the concrete play a major role in the damping. Greater water contents lead in general to larger damping. In [9], a damping ratio for water saturated specimen of  $\xi = 0.6$  to  $2.0\%$ , for partially saturated specimen of  $\xi = 0.9$  to  $1.8\%$ , and for dry specimen of  $\xi = 0.2$  to  $0.4\%$  are indicated. With increasing age of the concrete the damping in general initially decreases, possibly due to progressive drying. After three to four weeks drying time, however, the influence of the age of the concrete ceases to be significant.

#### 5. THEORETICAL FOUNDATIONS

For the description of the damping properties of a material respectively a construction, two characteristic values can be appropriately defined ([10], [11]):

- The damping energy dissipated per vibration cycle.
- The relationship between the damping energy and the maximal strain energy.

The total damping energy  $D_0$  is the energy which is dissipated in the entire test body respectively the entire construction during one vibration cycle [Nm/cycle]. The total damping energy  $D_0$  can be calculated from the specific damping energy  $D$  by integration over the volume  $V$  of the test body

$$D_0 = \int_V D \cdot dV \quad (1)$$

The specific damping energy  $D$  is that energy which is dissipated within a volume element respectively a volume at a definite point in the test body during a vibration cycle [Nm/cycle]. Under a linear (uniaxial) stress condition,  $D$  can in general be determined from the equation

$$D = d \cdot \left( \frac{\sigma}{\beta_p} \right)^n \quad (2)$$

where  $d$  = specific damping coefficient [N/mm<sup>2</sup>]  
 $\sigma$  = the maximal stress upon the volume element during the vibration  
 $\beta_p$  = cylinder strength of the concrete  
 $n$  = damping exponent.

Empirically, the value of  $n$  for low stresses lies between 1.0 and 3.0. For high stresses, however,  $n$  can be substantially greater than 3.0. It can be shown that the familiar models for the representation of the damping behavior are contained in this equation. For example, the value  $n = 2$  corresponds to viscous damping and the value  $n = 1$  corresponds to friction damping with constant frictional force (see [3]).

The specific damping energy  $D$  is the most fundamental of all the known used damping values since it is dependent only on the material studied and is not in-

fluenced by the form and the volume of the body or the existing stress distribution.

The maximal strain energy  $W$  respectively  $W_0$  of a volume element respectively of an elastic body under a linear (uniaxial) stress condition can be calculated from the equation

$$W = \frac{1}{2} \cdot \frac{\sigma^2}{E} \cdot dV, \quad \text{respectively} \quad W_0 = \frac{1}{2} \cdot \int_V \frac{\sigma^2}{E} \cdot dV \quad (3)$$

where  $\sigma$  = maximum stress upon the volume element during the vibration  
 $E$  = modulus of elasticity.

From the relationship of the damping energy  $D$  respectively  $D_0$  to the maximum strain energy  $W$  respectively  $W_0$ , the damping ratio  $\xi$  of the material respectively of a volume element and the damping ratio  $\xi_0$  of the entire test body can be calculated from

$$\xi = \frac{D}{4 \cdot \pi \cdot W}, \quad \text{respectively} \quad \xi_0 = \frac{D_0}{4 \cdot \pi \cdot W_0} \quad (4)$$

The damping ratio corresponds to the percent total of the maximum strain energy respectively vibration energy which is dissipated through damping during every vibration period. In general the relationship

$$\xi^{el} \neq \xi$$

is true because the damping energy  $D_0$  is determined not only by the material properties but also by the form of the test body and the stress condition.

For the calculation of a vibrator with one degree of freedom and nonlinear damping properties (no viscous damping), the so-called equivalent viscous damping is very frequently introduced. This makes it possible to simplify for calculation the damping properties of such a vibrator by a linear vibrator with viscous damping. The energy dissipation of the nonlinear vibrator is replaced by the equivalent viscous damping of the linear vibrator, with the equivalent viscous damping ratio  $\xi_{eq}$  of the linear vibrator so chosen that both vibrators dissipate the same energy  $D_0$  per vibrator period. For known damping energy  $D_0$  and strain energy  $W_0$ , the equivalent viscous damping ratio  $\xi_{eq}$  can be calculated from Equation (4).

The use of the damping ratio  $\xi$  for dynamic calculations has the following advantages:

- $\xi$  can be quickly established by simple tests.
- The damping is not dependent on the frequency of vibration (experimentally confirmed).
- The solution of the differential equation of vibration becomes especially simple.

## 6. PROCEDURE FOR THE DEVELOPMENT OF A DAMPING MODEL FOR A REINFORCED CONCRETE BEAM

Most uncracked and cracked zones for a reinforced concrete beam can appear during service condition. Therefore, since the crack condition of the beam has a very strong influence on its damping properties, the procedure for the development of a damping model was chosen according to the following basic ideas:

- First only small pieces of the beam, each consisting of either a cracked or an uncracked bending element, were considered. A damping model for each of these bending elements was defined.



- A complete reinforced concrete beam is built-up from a number of both cracked and uncracked bending elements, the exact number of each depending on the crack condition (see Fig. 5). Thus, the damping model for the complete beam can be found through suitable superposition of the damping properties of the separate bending elements.

This procedure has the following advantages:

- The influence of the different stresses along the length of the beam can be considered.
- The bond properties, which are important for the damping, can be included.
- By summation of the damping energy for the single bending elements, the damping energy for a totally uncracked, partially cracked or totally cracked beam can be determined.

Using the damping model for a bending beam, the experimentally determined results of [1] must be able to be explained. As a foundation for the damping model for an entire beam, the damping models for a bending element must be able to show the causes of the influence of

- crack growing
- amplitude respectively stress level
- reinforcement content

on the damping of normally-reinforced and also, if possible, prestressed concrete and light-weight concrete beams.

#### 7. DAMPING MODEL FOR AN UNCRACKED BENDING ELEMENT

Fig. 2 shows the damping model for an uncracked bending element. It consists of

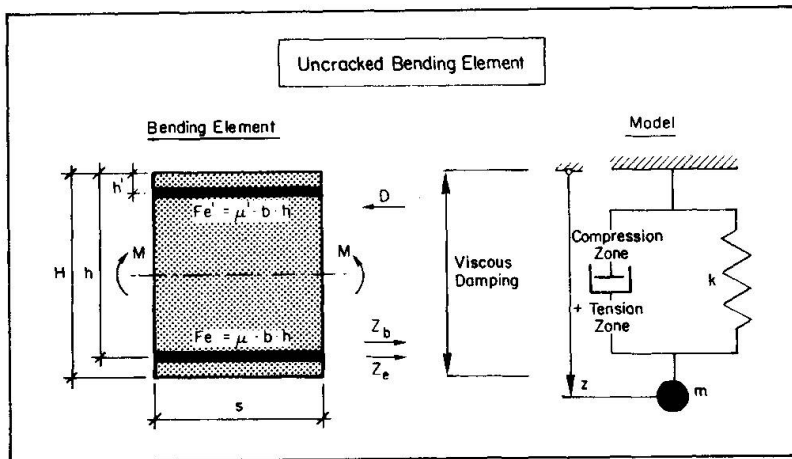


Fig. 2 Damping Model for an Uncracked Bending Element

one damping element with linear viscous damping, which contains the energy dissipated in the concrete bending compression zone as well as in the concrete bending tension zone. The energy dissipated in the reinforcement through stress under the yield level is comparatively small and is there neglected. The main reason for the use of the viscous damping model was that, in agreement with the conducted tests on the unreinforced concrete test bodies as well as those on fully-prestressed uncracked concrete beams, a damping

ratio independent of the height of the stress can be obtained ( $n = 2$ ,  $\xi = \text{const.}$ ; see Eq. (4)).

It is accepted in the following that an equal amount of energy is dissipated by equal-sized tension and compression stresses, so that both tension zone and compression zone contribute the same amount to the energy dissipated in a symmetrically reinforced beam. From Eqs. (1) and (2) with  $n = 2$ , the energy  $De_{O,VD}^{el}$  dissipated in an uncracked bending element (length  $s$ , width  $B$ , height  $H$ ) through viscous damping (VD) can be calculated by integration over the entire volume of the bending element. After the calculation of the maximum strain energy  $w_O^{el}$  collected



in the bending element, the damping ratio  $\xi_{VD}^{el}$  of the uncracked bending element corresponding to Eq. (4) can be calculated from

$$\xi_{VD}^{el} = \frac{d \cdot E_b}{2 \cdot \pi \cdot C_o \cdot \beta_p^2} \quad (5)$$

with

$$C_o = 1 + 3 \cdot n \cdot \frac{h}{H} \cdot (\mu + \mu') \cdot \left( \frac{\frac{H}{2} - h'}{\frac{H}{2}} \right)^2$$

$$n = \frac{E_e}{E_b}$$

The damping ratio  $\xi_{VD}^{el}$  is independent from the level of the stress and is determined besides the modulus of elasticity  $E_b$  and the cylinder strength  $\beta_p$  of the concrete mainly through the specific damping coefficient  $d$ . This coefficient depends on the material and must therefore be experimentally determined. The reinforcement ratio  $\mu$  respectively  $\mu'$  is considered in the coefficient  $C_o$ . Its influence on the damping ratio  $\xi_{VD}^{el}$  is relatively negligible.

## 8. DAMPING MODEL FOR A CRACKED BENDING ELEMENT

Fig. 3 shows the damping model for a cracked bending element. It is a combined

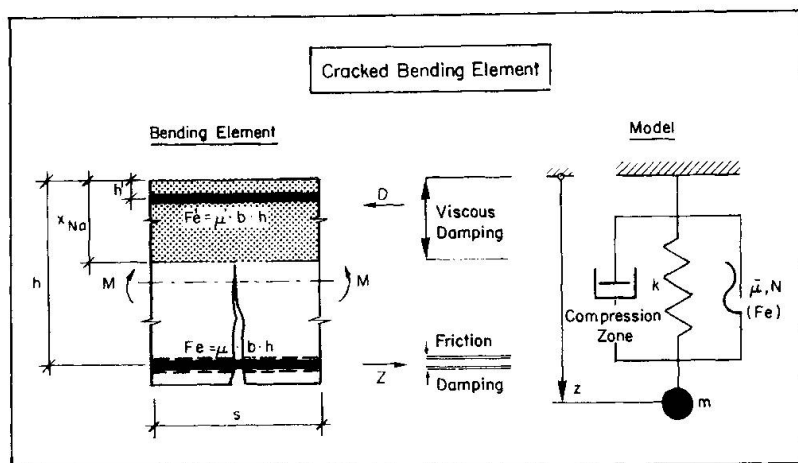


Fig. 3 Damping Model for a Cracked Bending Element

consideration of damping, only the friction damping model is capable of explaining the reduction of the damping ratio for growing stress ( $n = 1$ ,  $\xi \sim 1/\sigma$ , see Eq. (4)).

In the following it shall be shown that the assumptions of energy dissipation through friction damping for a cracked beam are fulfilled, in particular the existence of a normal force respectively a friction force and a corresponding displacement.

In the literature, a supposed friction damping is frequently explained by friction between the edges of the cracks. This statement is, however, too superficial. As long as the edges of the crack move in a direction perpendicular to the crack (opening and closing of the crack), no friction force can exist in the crack. The friction damping can exist, however, at the bond respectively the contact area between the concrete of the tension zone and the tension reinforcement.

### 8.1 Bond Between Reinforcement and Concrete

The bond relationship for ribbed reinforcement has been thoroughly described,

damping mechanism, consisting of two damping elements connected in parallel to a spring element. With the linear viscous damping of the first damping element, the portion of the damping which was established in all tests to be independent of the level of stress can be considered (see Fig. 1). The friction damping of the second element carries that portion established to be dependent on the level of the amplitude respectively the stress and the reinforcement ratio. Of the current models used for the





exemples being [12], [13] and [14]. It has been successfully established that the transfer of the tension forces from the reinforcement to the concrete has two results. First, there are radial stresses  $\sigma_r$  working perpendicular to the reinforcement axis and causing a tension ring stress  $\sigma_{rz}$  in the concrete. Second, the reinforcement experiences a displacement  $v$  relative to the concrete.

Fig. 4 shows how the rib force  $P_R$  of the reinforcement is taken up by the concrete through compression and tension forces (corresponding to  $\sigma_r$  and  $\sigma_{rz}$ ).

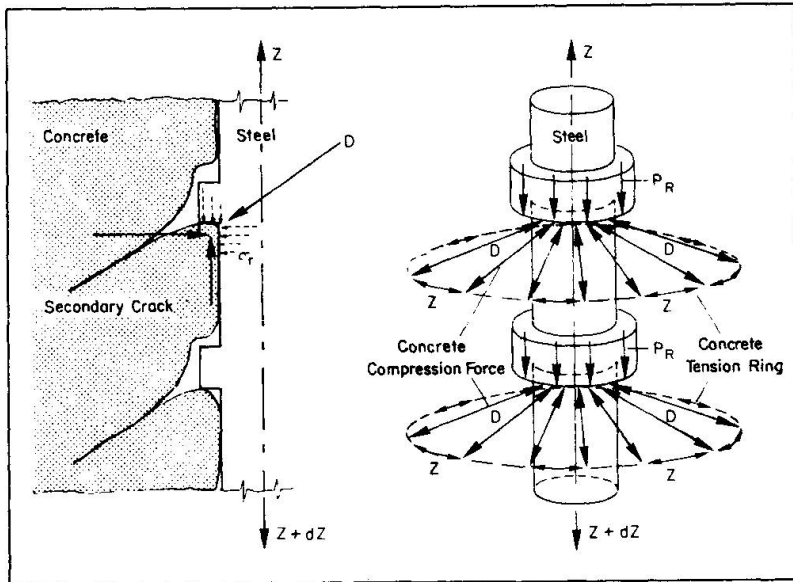


Fig. 4 Spreading of the Bond Stresses  $\tau_v$ , resp. Ribbing Forces  $P_R$

As a result of the load by the rib force  $P_R$ , cracks (secondary cracks) are developed in the surrounding concrete near to every rib. These cracks determine the inclination of the compression force  $D$  and consequently the size of the radial stress  $\sigma_r$ . The cracks are in general not visible on the surface of the concrete.

The bond stress  $\tau_v$  is a hypothetical value with which the effective existing forces between the reinforcement rib and the concrete as well as the friction forces between the steel and the covering concrete can be simplified and included. In [12] are given theoretical relation-

ships as well as a relationship experimentally determined for small bodies concerning the bond stress  $\tau_v$  and the displacement  $v$  of the reinforcement relative to the concrete (bond law). Using these relationships, the distribution of the bond stress  $\tau_v$  can be calculated, and therefore also the radial stress  $\sigma_r$  and the relative displacement  $v$  along the reinforcement axis. Using the now assumed-to-be-known distribution of the bond stress  $\tau_v$  respectively the radial stress  $\sigma_r$  and the relative displacement  $v$  along the reinforcement axis, the friction force  $F_{FD}$  on the bending element and the corresponding relative displacement  $v$  and from these the energy dissipated through friction damping can be calculated.

## 8.2 Energy Dissipation through Viscous Damping

In contrast to the uncracked bending element (see Fig. 2), only the bending compression zone shall dissipate energy appropriate to the viscous damping model. The energy dissipated through viscous damping in the bending tension zone and the reinforcement shall be neglected, since the contribution of the bending tension zone to the damping energy, due to its comparatively smaller stresses, is significantly smaller than the contribution of the bending compression zone (see Eq. (2)). The damping energy  $D_{O,VD}^{el}$  can now be calculated from Eq. (1) by integration over the volume of the bending compression zone. After determination of the strain energy  $W_O^{el}$ , the damping ratio  $\xi_{VD}^{el}$  as a result of viscous damping becomes

$$\xi_{VD}^{el} = \frac{6 \cdot E_b}{3 \cdot 4 \cdot \pi} \cdot \frac{d \cdot B \cdot x_{Na} \cdot s \cdot \sigma_b^2}{C_1 \cdot B \cdot x_{Na} \cdot s \cdot \sigma_b^2 \cdot \beta_p^2} = \frac{d \cdot E_b}{2 \cdot \pi \cdot C_1 \cdot \beta_p^2} \quad (6)$$

with 
$$C_1 = 1 + 3 \cdot n \cdot \mu \cdot h \cdot \frac{(h - x_{Na})^2}{x_{Na}^3} + 3 \cdot n \cdot \mu' \cdot h \cdot \frac{(x_{Na} - h')^2}{x_{Na}^3} .$$

A comparison of Eqs. (5) and (6) shows that the expressions for viscous damping for an uncracked and a cracked bending element differ only in regard to  $C_0$  and  $C_1$ .

### 8.3 Energy Dissipation through Friction Damping

In order to be able to calculate the energy  $D_{O,FD}^{el}$  dissipated by friction damping in a cracked bending element,

- the coefficient of sliding friction  $\bar{\mu}(x,t)$ ,
- the normal force  $N(x,t)$  respectively the radial stress  $\sigma_r(x,t)$ ,
- the relative displacement  $v(x,t)$

between the concrete and the reinforcing steel must be known for all times and locations. However, by using the following assumptions and simplifications, the damping energy  $D_{O,FD}^{el}$  can be easily calculated.

- Coefficient of sliding friction  $\bar{\mu}$  constant over time and location.
- Linear relationship between bond stress  $\tau_v(x,t)$  and radial stress  $\sigma_r(x,t)$ :

$$\sigma_r(x,t) = A \cdot \tau_v(x,t) \quad (7)$$

with  $A$  = proportionality factor

- Linear relationship in the cracked cross section between the relative displacement  $v_{max}(t)$  (between the reinforcement and the concrete) and the steel stress  $\sigma_{e,max}(t)$ .
- Independence of the bond stress  $\tau_v$  respectively the radial stress  $\sigma_r$  from the level of the steel stress respectively the stress ( $\tau_v = \text{const.}$ ).

With these simplifications, whose justification is thoroughly discusses in [3], the friction force  $F_{FD}^{el}$  for a cracked bending element with  $j$  reinforcement bars of diameter  $\phi$  becomes

$$F^{el} = \pi \cdot \phi \cdot j \cdot \bar{\mu} \cdot A \cdot \tau_v \cdot s \quad (8)$$

The damping energy  $D_{O,FD}^{el}$  dissipated through friction damping for a harmonically vibrating bending element can be calculated from

$$D_{O,FD}^{el} = 4 \cdot F_{FD}^{el} \cdot v_m \quad (9)$$

where  $v_m$  = the average relative displacement over the length of the bending element.

Using this equation, the damping ratio  $\xi_{FD}^{el}$  as a result of friction damping becomes

$$\xi_{FD}^{el} = \frac{4 \cdot F_{FD}^{el} \cdot v_m}{4 \cdot \pi \cdot W_O} = \text{constant} \cdot \frac{\sigma_{e,max}}{\sigma_{e,max}^2} \quad (10)$$

Since the average relative displacement corresponding to the stated simplification increases linearly with the steel stress, the damping ratio  $\xi_{FD}^{el}$  is inversely proportional to the steel stress. It can be shown that the crack interval  $s$  (that is the length of the bending element) has only a small influence on the damping ratio  $\xi_{FD}^{el}$



#### 8.4 Combination of Viscous Damping and Friction Damping

The damping ratio for a cracked bending element corresponds to the sum of the damping energies for viscous damping and friction damping, and is composed of the sum of the damping ratio for viscous damping and friction damping:

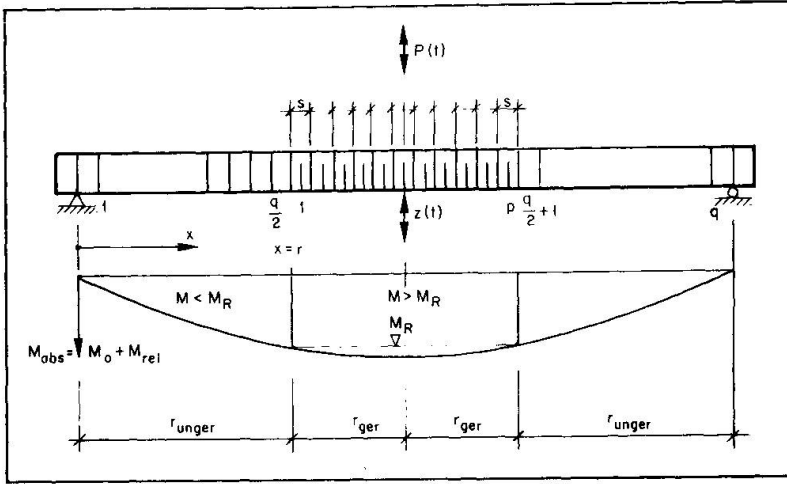
$$\xi^{el} = \xi_{VD}^{el} + \xi_{FD}^{el} \quad (11)$$

$$\xi^{el} = \frac{d \cdot E_b}{2 \cdot \pi \cdot C_1 \cdot \beta_p^2} + \frac{6 \cdot n^2 \cdot E_b \cdot \bar{\mu} \cdot A \cdot j \cdot \phi \cdot \tau_v \cdot v_m(\sigma_{e,max})}{C_2 \cdot B \cdot h \cdot \sigma_{e,max}^2}$$

$$\text{with } C_2 = \frac{x_{Na}^3}{3 \cdot h \cdot (h - x_{Na})^2} + n \cdot \mu + n \cdot \mu' \cdot \left( \frac{x_{Na} - h'}{h - x_{Na}} \right)^2$$

#### 9. DAMPING MODEL FOR A REINFORCED CONCRETE BEAM

Fig. 5 shows a partially cracked, simply-supported reinforced concrete beam.



With the shown bending moment, the cracks due to bending will appear first in the center of the beam. These cracks can be represented by a corresponding number of uncracked (q) and cracked (p) bending elements which depend upon the crack condition of the beam. The damping properties of each uncracked and cracked bending element can be determined with help of the previous section. The damping model for the entire beam is then obtained by a suitable summation of the damping

Fig. 5 Partially-Cracked Reinforced Concrete Beam

properties of each bending element. Following as an example the damping properties of a simply-supported beam (see Fig. 5) are calculated.

The damping ratio  $\xi$  for a perfectly cracked beam ( $r = l/2$ ) can be calculated from

$$\xi = \xi_{VD} + \xi_{FD}$$

$$\xi = \frac{d \cdot E_b}{2 \cdot \pi \cdot C_1 \cdot \beta_p^2} + \frac{24 \cdot n^2 \cdot \bar{\mu} \cdot A \cdot j \cdot \phi \cdot E_b \cdot \tau_v \cdot v_m(\sigma_{e,d})}{\pi \cdot h \cdot B \cdot C_2 \cdot \sigma_{e,d}^2} \quad (12)$$

where  $\sigma_{e,d}$  = maximum steel stress in the middle of the beam.

Fig. 6 shows the damping ratio  $\xi$  as a function of the amplitude  $z$  respectively the steel stress  $\sigma_{e,d}$ . The first term is independent of the level of the steel stress respectively stress. The second term is inversely proportional to this steel stress due to the linear relationship between the relative displacement  $v$  and the steel stress  $\sigma_e$ . For small dynamic amplitudes respectively stresses, the damping ratio will be relatively large. For growing amplitudes respectively stresses, the damping ratio  $\xi$  will approach the damping ratio  $\xi_{VD}$  due to the viscous damping.

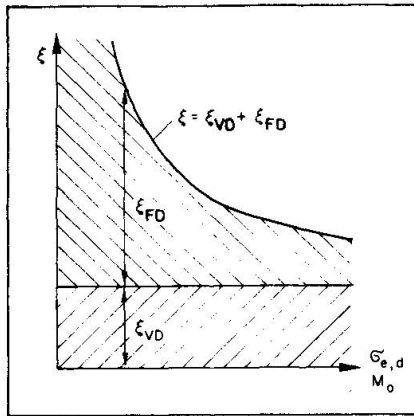


Fig. 6 Damping Ratio  $\xi$  as a Function of the Stress for a Fully-Cracked Reinforced Concrete Beam

An uncracked beam ( $r = 0$ ) dissipates energy only through viscous damping, which makes the damping ratio  $\xi_{VD}$  relatively small. Raising the bending stress over the crack moment  $M_R$  results in a very quick formation of numerous cracks, beginning in the beam middle. Every increase in the number of cracked bending elements results in a increase in the number of elements with friction damping. This effect causes initially a sharp increase in the damping ratio  $\xi = \xi_{VD} + \xi_{FD}$ . The growth of the cracked zone slows with further increasing stresses. If the friction force  $F_{FD}$  for increasing stress continues to slowly increase, the damping ratio  $\xi_{FD}$  will fall after reaching a maximum value. This effect appears since the influence of the amplitude-dependent friction damping (see Eq. 10)) overweighs the influence of the growing friction force.

## 10. NUMERICAL VALUES AND COMPARISON WITH EXPERIMENTAL RESULTS

It shall now be shown that the described damping model for uncracked and cracked bending elements respectively an entire reinforced concrete beam can be correctly applied to show the real relationships in experimentally tested beams.

### 10.1 Basic Parameters

#### a) Viscous Damping

The analysis of numerous reinforced concrete beams and concrete specimens brought the result that the damping ratio  $\xi_{VD}^{el}$  for concrete and light-weight concrete can be established in practically all cases as follows:

$$\begin{aligned} \text{Normal concrete} & : \quad \xi_{VD} = 0.006 \\ \text{Light-weight concrete with} & \\ \text{aggregates of expanded clays} & : \quad \xi_{VD} = 0.005 \end{aligned} \quad (13)$$

In these statements, the influence factors for the damping relationships of unreinforced concrete respectively light-weight concrete, namely

- the water content
- the age

although described as important, are not taken into account. This simplification may be made in designed construction, which includes nearly all structures for which a dynamic analysis must be made, for the following two reasons. First, most concretes respectively light-weight concretes used have similar water-cement ratios (0.45 to 0.50). Second, the age of the concrete noticeably influences the damping properties only in the first weeks following placement.

#### b) Friction Damping

A large degree of uncertainty exists concerning the size of the coefficient of sliding friction  $\bar{\mu}$  and the proportionality coefficient  $A$  (see Eq. (7)). The product  $\bar{\mu} \cdot A$  for the test beams described in [10] can be determined with help of Eq. (8). The value for the product  $\bar{\mu} \cdot A$  varies for all test beams within the small range of

$$0.01 \leq \bar{\mu} \cdot A \leq 0.03 \quad (14)$$



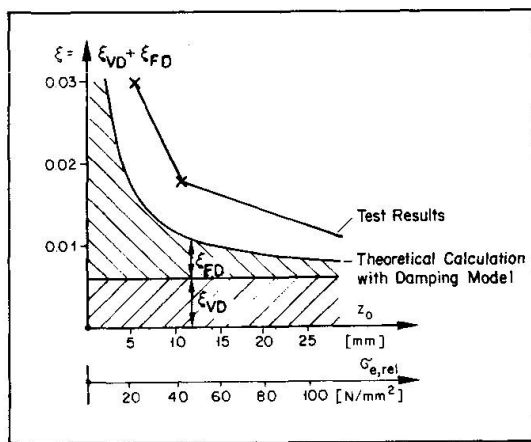
This means that the friction force  $F_{FD}$  produced by the steel used in these experiments (Torstahl) amounts to between 1% and 3% of the average force transferred from the steel to the concrete due to the bond stress. Additionally it can be established that the product  $\bar{\mu} \cdot A$  would become smaller for increasing test duration. It appears that the coefficient of sliding friction  $\bar{\mu}$  decreases with time due to the large number of load changes and the high stress changes.

## 10.2 Comparison of the Results of the Damping Model with the Experimental Results

As an example, the damping properties of beam B3 (see [1]) due to the described damping model will be compared to the corresponding test results. The detailed procedure and the derivation of the theoretical results are described in [3].

For  $\xi_{VD} = 0.006$  and  $\bar{\mu} \cdot A = 0.015$ , the amplitude-dependent damping ratio  $\xi$  becomes

$$\xi = \xi_{VD} + \xi_{FD} = 0.006 + 0.0572 \cdot \frac{1}{z_0} \quad (15)$$



The resulting course of  $\xi$  as a function of the amplitude  $z_0$  obtained from Eq. (15) is shown in Fig. 7.

The comparison of these results with the experimental results (also shown in Fig. 7) shows a good agreement between experiment and theory.

Fig. 8 shows in solid lines the resonance curves developed during a stress level with rising and falling applied frequencies.

Fig. 7 Test Beam B3, Damping Ratio  $\xi$  as a Function of Amplitude  $z_0$

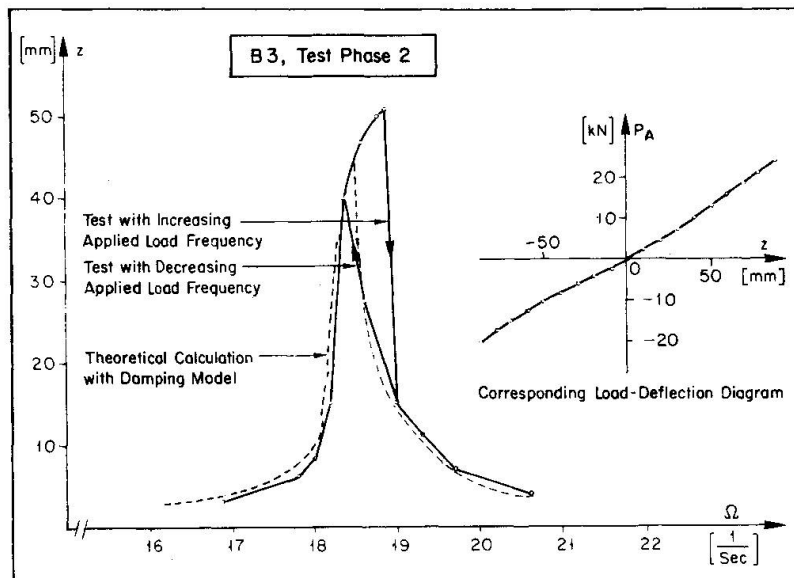


Fig. 8 Test Beam B3, Comparison of a Theoretically Calculated Resonance Curve ( $F_{FD} = \text{const.}$ , indicated Load-Deflection Diagram) with Test Results

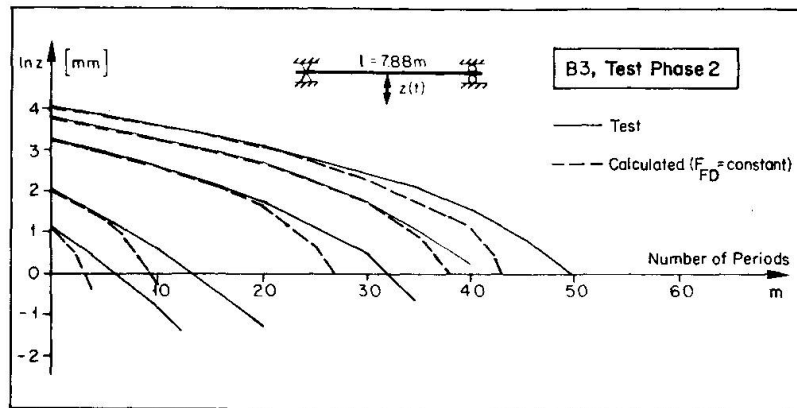


Fig. 9 Test Beam B3, Amplitudes for various Free Vibration Tests, Test Results and Theoretically Calculated Results ( $F_{FD} = \text{constant}$ )

Fig. 9 shows through solid lines the amplitudes established by numerous tests. On the abscissa is the number of vibration periods  $m$ , and on the ordinate is the logarithm of the maximum amplitude  $z$  achieved by free vibration test after  $m$  periods.

Also shown in Figs. 8 and 9 through dashed lines are the amplitudes calculated for a constant friction force  $F_{FD}$  (see Eq. (8)).

A comparison of the corresponding lines shows that the calculated amplitudes agree very well with the experimental results.

It is shown in [3] that by using the effective course of the bond stress  $\tau_v$  calculated due to the differential equation of bond, that is by using  $F_{FD} \neq \text{const.}$ , a still better agreement between the experimental and the theoretical results can be achieved.

## 11. LIMITS OF APPLICATION

The previously described damping model may not be used in the dynamic analysis of the following cases without further testing:

- For very high stresses of the concrete (i.e.  $\sigma_b > \beta_w/2$ ) and the reinforcement steel (i.e.  $\sigma_e > 0.7 \cdot \sigma_{e,2.0}$ ), an important portion of the total damping energy is dissipated by hysteretical damping (energy dissipation through nonlinear material relationships) which is not considered by the damping model. The damping can amount to a multiple of the damping for small stresses.
- The damping model was developed for use with normally reinforced concrete beams, but is also presumed allowable for use with partially-prestressed and cracked concrete beams. The experimental justification is not considerable, however.
- Depending on the statical system, the type of supports and the building site, the not included system damping can have an important or even a dominating effect on the total damping of a structure. Most significantly, very stiff structures with fixed supports can have a very large system damping. On the contrary, it appears that thin structures with hinged supports and low-friction rollers or sliding supports show almost no material damping.
- For a concrete structure which is predominately stressed by shear and torsion, a damping relationship analogous to that for bending stress is expected. It is also supposed for the case that the total material damping will be composed partly of viscous damping and partly from friction damping. The friction damp-





ing can again be limited mainly to the friction between the stirrups respectively the longitudinal reinforcement and the surrounding concrete. However, a displacement in the direction of the shear crack appears in addition to the movement perpendicular to the crack edges. Due to the interlocking of the crack edges, the shear resistance can on the one hand be increased. On the other hand, it is also now possible that due to the relative displacement of the interlocked and no longer stress-free crack edges, energy can be dissipated by friction damping.

#### REFERENCES

- 1 Dieterle R., Bachmann H.: "Versuche über den Einfluss der Rissbildung auf die dynamischen Eigenschaften von Leichtbeton- und Betonbalken", Institut für Baustatik und Konstruktion, ETH Zürich, Versuchsbericht Nr. 7501-1, Birkhäuser Verlag Basel und Stuttgart, Dezember 1979.
- 2 Dieterle R., Bachmann H.: "Einfluss der Rissbildung auf die dynamischen Eigenschaften von Leichtbeton- und Betonbalken", Schweizer Ingenieur + Architekt, 98. Jahrgang, Heft 32/80, 7.8.1980.
- 3 Dieterle R.: "Modelle für das Dämpfungsverhalten schwingender Stahlbetonträger im gerissenen und ungerissenen Zustand", ETH Zürich, Dissertation Nr. 6768, Institut für Baustatik und Konstruktion, Zürich 1981.
- 4 Swamy R.N.: "Damping Mechanisms of Cementitious Systems", Chapter 30 in 'Dynamic Waves in Civil Engineering', Wiley Interscience, 1974.
- 5 Girgrah M., Kesler C.E.: "A Study of the Rheological and Damping Properties of Concrete", Theoretical and Applied Mechanics, Report No. 173, University of Illinois, Urbana, Ill., 1960, p 53 ff.
- 6 Jones R.: "The Effect of Frequency on the Dynamic Modulus and Damping Coefficient of Concrete", Zement-Kalk-Gips, Nr. 7, 1958, p. 321-322.
- 7 Ehlers G.: "Das Elastizitätsmass des Betons bei Schwingungen", Beton und Eisen, Heft 20, 1941.
- 8 Kesler C.E., Higuchi Y.: "Determination of Compressive Strength of Concrete by Using its Sonic Properties", Proceedings of ASTM, Vol. 53, 1953, p. 1044.
- 9 Richards C.W., Radjy F.: "A New Application of Internal Friction to Concrete Research", Materials Research and Standards, Vol. 6, No. 8, August 1966, p. 386-392.
- 10 Goodman L.E.: "Material Damping and Slip Damping", Chapter 36 in 'Shock and Vibration Handbook', MacGraw-Hill Book Company, Inc., New York, 1961.
- 11 Lazan B.J.: "Internal Friction, Damping and Cyclic Plasticity", ASTM Special Technical Publication No. 378, 1965.
- 12 Rehm G.: "Ueber die Grundlagen des Verbundes zwischen Stahl und Beton", Deutscher Ausschuss für Stahlbeton, Heft 138, Berlin, 1961.
- 13 Martin H.: "Zusammenhang zwischen Oberflächenbeschaffenheit, Verbund und Sprengwirkung von Bewehrungsstählen unter Kurzzeitbelastung", Deutscher Ausschuss für Stahlbeton, Heft 228, Berlin, 1973.
- 14 Goto Y.: "Experimental Studies on Cracks Formed in Concrete around Deformed Tension Bars", Technology Reports, Tohoku University, Vol. 44, N.1, 1979.